RESEARCH ARTICLE

SARS-CoV-2 nucleocapsid protein enhances the level of mitochondrial reactive oxygen species

Haiyun Yu[1] | Lu Yang[1] | Zhennan Han[1] | Xiaoyu Zhou[1] | Zihan Zhang[1] | Tianli Sun[1] | Fang Zheng[2] | Jingzhi Yang[3] | Fei Guan[1] | Jungang Xie[4] | Chaohong Liu[1]

[1]Department of Pathogen Biology, School of Basic Medicine, Tongji Medical College and State Key Laboratory for Diagnosis and Treatment of Severe Zoonotic Infectious Diseases, Huazhong University of Science and Technology, Wuhan, Hubei, China

[2]Department of Immunology, School of Basic Medicine, Tongji Medical College, Huazhong University of Science and Technology, Wuhan, Hubei, China

[3]Department of Orthopedics, Qilu Hospital of Shandong University, Jinan, Shangdong, China

[4]Department of Respiratory and Critical Care Medicine, National Clinical Research Center of Respiratory Disease, Tongji Medical College, Tongji Hospital, Huazhong University of Science and Technology, Wuhan, China

Correspondence
Chaohong Liu, Department of Pathogen Biology, School of Basic Medicine, Tongji Medical College and State Key Laboratory for Diagnosis and Treatment of Severe Zoonotic Infectious Diseases, Huazhong University of Science and Technology, Wuhan, Hubei, China.
Email: chaohongliu80@126.com

Funding information
National Natural Science Foundation of China, Grant/Award Number: 82371784; College Students' Innovative Entrepreneurial Training Plan Program, Grant/Award Number: 202210487079; R&D Program of Guangzhou Laboratory, Grant/Award Number: SRPG22-006; HUST Academic Frontier Youth Team, Grant/Award Number: 2018QYTD10

Abstract

Coronavirus disease 2019 (COVID-19) pathogenesis is influenced by reactive oxygen species (ROS). Nevertheless, the precise mechanisms implicated remain poorly understood. The nucleocapsid (N) protein of severe acute respiratory syndrome coronavirus 2 (SARS-CoV-2), the main driver for this condition, is a structural protein indispensable for viral replication and assembly, and its role in ROS production has not been reported. This study shows that SARS-CoV-2 N protein expression enhances mitochondrial ROS level. Bulk RNA-sequencing suggests of aberrant redox state of the electron transport chain. Accordingly, this protein hinders ATP production but simultaneously augments the activity of complexes I and III, and most mitochondrially encoded complex I and III proteins are upregulated by it. Mechanistically, N protein of SARS-CoV-2 shows significant mitochondrial localization. It interacts with mitochondrial transcription components and stabilizes them. Moreover, it also impairs the activity of antioxidant enzymes with or without detectable interaction.

KEYWORDS
interaction, mitochondria, nucleocapsid, ROS, SARS-CoV-2

1 | INTRODUCTION

Coronavirus disease 2019 (COVID-19), caused by severe acute respiratory syndrome coronavirus 2 (SARS-CoV-2), has led to widespread suffering. Reactive oxygen species (ROS) has been hypothesized to be the major mediator of SARS-CoV-2-induced pathogenesis.[1–3] Mitochondria serve as the primary sites for ROS production. The generation of mitochondrial ROS is contingent upon the electron transport chain redox state, with complexes I and III playing particularly significant roles.[4,5] Besides, the activation of β-nicotinamide adenine dinucleotide phosphate (NADPH) oxidase within plasma membranes leads to ROS production in various cells

and tissues such as macrophages, neutrophils, cardiomyocytes, endothelial cells, and vascular smooth muscle cells.[4,5] ROS production is usually controlled by three types of antioxidant enzymes: catalase (CAT), superoxide dismutases (SODs), and glutathione peroxidases (Gpxs).[4,5]

The SARS-CoV-2, a β-coronavirus family constituent, is characterized by its non-segmented, enveloped, positive-sense, single-stranded RNA. Its ~30 kb viral genome can lead to the production of the 16 nonstructural proteins (Nsp), nine putative accessory proteins, and four structural proteins, that is, membrane (M), envelope (E), Spike (S), and nucleocapsid (N) proteins.[6] The virus fuses with the host cell membrane when the transmembrane serine protease 2 cleaves the S protein, activating it and causing it to engage with angiotensin-converting enzyme 2.[7] Consequently, S protein inhibits the ability of angiotensin-converting enzyme 2 to convert angiotensin II into angiotensin 1–7, a physiological antagonist of angiotensin II.[8] As angiotensin II potently activates NADPH oxidase, S protein enhances ROS production through angiotensin II-mediated over-activation of NADPH oxidase.[9] However, whether other SARS-CoV-2-encoded protein also enhances the level of ROS remains elusive.

The N protein of human-infecting coronaviruses is usually produced at high levels in infected cells and is indispensable for viral replication and assembly.[10,11] There is accumulating evidence suggesting that SARS-CoV-2 N protein (S2NP) is multifunctional. Through RNA-induced liquid–liquid phase separation and interaction with various host cellular proteins, this protein is crucial in the pathogenesis of COVID-19.[12] Its role in ROS production has not been reported. This study shows that the expression of S2NP enhances the level of mitochondrial ROS through, at least partially, binding to mitochondrial transcription components and stabilizing them.

2 | MATERIALS AND METHODS

2.1 | Cellular culturing, transfection/transduction

Human lung carcinoma cells (A549) were procured from the Shanghai Institute for Biological Sciences. HBE human bronchial epithelial cells were from Jungang Xie's laboratory in Tongji Hospital, Tongji Medical College, Huazhong University of Science and Technology. These cells were grown within Dulbecco's modified Eagle's medium augmented through 10% fetal bovine serum, 100 U/mL penicillin, together with 100 μg/mL streptomycin at 37°C with 5% CO_2. The mammalian expression plasmid encoding S2NP was constructed by cloning synthetic DNA (GeneBank: MN908947.3) into a pEGFP-N1 vector. Lipofectamine 2000 (Invitrogen) at a ratio of 1:1 was used for plasmid transfection. Recombinant adenovirus type-5 (Ad5) expressing FLAG-tagged S2NP (Ad5-N) (GeneBank: MN908947.3) or empty vectors were obtained from Vigenebio.[13] Adenovirus transduction was conducted in line with kit methodology recommendations.

2.2 | Mitochondrial ROS staining

Mitochondrial ROS was measured with MitoSOX™ red reagent (M36008; Invitrogen). Briefly, Ad5- or Ad5-N-transduced cells were incubated with 0.5 μM MitoSOX™ red reagent for 30 min at 37°C and 5% CO_2 in magnesium and calcium containing warm HBSS. After washing with the HBSS mentioned above three times, cultures were exposed to 0.25% trypsin, followed by flow cytometry analysis using the Becton Dickinson™ FACS-Calibur® platform (BD Biosciences™).

2.3 | Immunoblotting (IB) and coimmunoprecipitation (co-IP)

IB and co-IP were carried out in RIPA buffer (50 mM Tris-Cl, pH 7.5, 1% TritonX-100, 1% sodium deoxycholate, 150 mM NaCl, 0.1% SDS, 2 mM sodium pyrophosphate, 25 mM β-glycerophosphate, 1 mM EDTA, with the phosphatase and protease inhibitor cocktail) and IP lysis buffer (10 mM Tris-HCl, 1% NP40, 150 mM NaCl, 2 mM EDTA, pH 7.5, with phosphatase and protease inhibitor cocktail), respectively, as previously described.[14,15] Antibodies against β-tubulin (T8328) and FLAG-tag (F1804) were ordered through Sigma-Aldrich™, antibodies for CAT (A18018), SOD1 (A0274), MT-CYB (A17966), MT-ND1 (A5250), MT-ND2 (A17968), MT-ND3 (A17969), MT-ND4 (A9941), together with MT-ND6 (A17991) were ordered from Abclonal Biotech. Antibodies against β-actin (81115-1-RR), NRF2 (80593-1-RR), Gpx8 (16846-1-AP), together with TFAM (22586-1-AP) were bought through Proteintech™. Antibody against MT-ND4L (abs139195) was purchased from Absin. Antibodies against phospho-JNK (Thr183/Tyr185, 4668), phospho-p38 (Thr180/Tyr182, 4511), together with TFB2M (50837) were obtained through Cell Signaling Technology™. Antibody against ETFA (GTX105155) was obtained from GeneTex.

2.4 | Indirect immunofluorescence analysis

A549 and HBE cells expressing GFP-tagged S2NP underwent fixing using 4% (w/v) paraformaldehyde (15 min at 25°C) and were subsequently rendered permeable through 0.5% Triton X-100 (15 min at 25°C). Once nonspecific sites were blocked using 1% bovine serum albumin (1 h at 25°C), cultures were placed into incubation with an anti-Tom20 antibody (sc-11415; Santa Cruz Biotechnology™) diluted within blocking buffer overnight at 4°C. Cultures were thrice-rinsed using 0.05% Tween 20 in PBS, followed by a 45 min incubating period in the presence of TRITC-conjugated goat anti-mouse IgG (at 25°C). Following additional washing as previously described, cells were placed into incubation with 1 μg/mL 4′,6-diamidine-2-phenylindole (DAPI), subsequently being observed using laser scanning confocal microscopy (RADIANCE 2100; Bio-Rad).

2.5 | Bulk RNA-sequencing

Total RNA in Ad5- or Ad5-N-transduced A549 cells was extracted with TRIzol reagent. Then bulk RNA-sequencing was conducted according to previous studies.[16] In brief, 1 µg total RNA with RNA integrity number >7.0 was used to purify poly(A) RNA. Sequencing libraries were generated using NEBNext® UltraTM RNA Library Prep Kit for Illumina® (NEB) following manufacturer's recommendations and index codes were added to attribute sequences to each sample. Subsequently, Illumina NovaseqTM 6000 (LC-Bio Technology™) was used for 2 × 150 bp paired-end sequencing. Raw data (raw reads) of fastq format were first processed through in-house perl script. After mapping reads for reference genome *Homo sapiens* Ensembl v96 using HISAT2 (v2.0.5) package, featureCounts v1.5.0-p3 was used to count the reads numbers mapped to each gene. FPKMs (total_exon_fragments/mapped_reads [millions] × exon_length [kB]) were calculated. Differential expression analysis of two conditions was performed using the edgeR R package (3.18.1). The *p* values were adjusted using the Benjamini & Hochberg method. Corrected *p*-value of 0.05 and absolute fold change of 2 were set as the threshold for significantly differential. Gene ontology (GO) biological process (BP) terms of these differentially expressed genes (DEGs) were annotated (corrected *p*-value less than 0.05) by the clusterProfiler R package, in which gene length bias was corrected. The sequencing data have been submitted to the GEO database with an accession number GSE231733 and reviewer token cdojmwokrzkjfgr.

2.6 | Quantitative RT-PCR

The total RNA of Ad5- or Ad5-N-transduced A549 cells were extracted by Trizol (Invitrogen), and reverse-transcribed with AB-Script III RT Master Mix (Abclonal). Then the synthetic cDNA was examined for the expression of transcription levels of different genes with 2 × Universal SYBR Green Fast qPCR Mix (Abclonal). The C_t value was used to aseess the gene expression by the $2^{-\Delta\Delta C_t}$ method. Fold amplification was normalized by *ACTB*. The appropriate primer sequences for the target genes are show in Supporting Information S1: Table 1.

2.7 | Measurement of ATP production

ATP production in Ad5- or Ad5-N-transduced A549 cells was measured with the ATPlite™ assay system (6016943; PerkinElmer). Briefly, adding mammalian cell lysis solution inactivates the endogenous ATPases by raising the pH of the cell culture medium. A substrate solution, which includes Luciferase and a mixture of several substances, is added, lowering the pH. Consequently, Luciferase catalyzes the reaction between ATP and D-Luciferin to produce long-lived luminescent signal. ATP level is positively correlated with the luminescence value.[17]

2.8 | Isolation of mitochondria

Resuspend Ad5- or Ad5-N-transduced A549 cells digested from a 6 cm dish in 1 mL hypotonic buffer (2 mM HEPES, 70 mM sucrose, 220 mM mannitol, 0.1 mM EDTA, 1% bovine serum albumin) and permit cells to swell on ice for 15 min. Pass cell suspension through a 22 gauge needle 15–20 times until most cells are single and stained by trypan blue. Centrifuge samples at 3000 rpm and 4°C for 5 min. Transfer supernatants into prechilled fresh tubes and centrifuge samples (13 600*g*/15 min/4°C). Pellets containing mitochondria together with supernatants are cytosol. After being washed twice in hypotonic buffer, mitochondria were subjected to IB or the measurement of complex III activity.

2.9 | Measurement of complex I and III activity

The activity of complexes I and III was measured with commercial kits (ab109721; ab109905; Abcam). Complex I function is monitored through NADH oxidation into NAD$^+$, and a dye's simultaneous reduction drives enhanced absorbance (450 nm). Couple complex II + III function rate is assessed through observing conversion levels for oxidized cytochrome *c* into reduced form, leading to increased absorbance at 550 nm.

2.10 | Measurement of CAT, SOD, or Gpx activity

The activity of antioxidant enzymes in Ad5- or Ad5-N-transduced A549 cells was assessed through commercially-available kits from Nanjing Jiancheng Bioengineering Institute. The basis of such measurements is stated as below. First, the hydrogen peroxide reduction by CAT can be rapidly stopped by ammonium molybdate. Ammonium molybdate reacts with the residual hydrogen peroxide to produce a yellowish complex, which results in the absorbance at 405 nm.[18] Second, xanthine oxidase catalyzes the reaction between WST-1 and superoxide anions to produce the water-soluble formazan dye, which results in the absorbance at 450 nm. SODs inhibit the reaction via the disproportionation of superoxide anions.[19] Third, reduced glutathione reacts with dinitrobenzoic acid to produce the yellow-color 5-thio-dinitrobenzoic acid anion, which leads to the absorbance at 412 nm. Gpxs catalyze the hydrogen peroxide reduction, oxidizing reduced glutathione. Hydrogen peroxide can consume reduced glutathione without the catalysis of Gpxs. So Gpx activity is negatively correlated with OD412 values after non-enzymatic reaction is subtracted.[20]

2.11 | Ubiquitination assay

Ad5- or Ad5-N-transduced A549 cultures were exposed to 20 µM MG132 (dissolved in DMSO, C2211; Sigma-Aldrich) or an equivalent DMSO level for 6 h. Cells were then solubilized in modified lysis buffer containing 1% SDS, as previously described.[14] The samples were sonicated post-incubation (60°C/10 min), with consequent dilution 10

times using modified lysis solution devoid of SDS. The cell lysates underwent centrifuging (4°C/13 600*g*/30 min) after being incubated at 4°C for 1 h with rotation. The amount of protein utilized for IP was 1 mg/sample. IB was performed after five washes of immunoprecipitated proteins in a washing buffer containing 0.1% SDS.

2.12 | Statistical analyses

The quantitative data sets reflected means ± standard deviations, assessed through Prism® 6.0 (GraphPad™). Student's *t*-test compared the difference across both cohorts. $p < 0.05$ was deemed to confer statistical significance.

3 | RESULTS

3.1 | S2NP expression enhances the level of mitochondrial ROS

To explore whether S2NP affects mitochondrial ROS, a cell-permeable fluorogenic dye MitoSOX™ was used. To mimic the abundant expression of human-infecting coronavirus N protein in infected cells, replication-deficient recombinant human adenovirus type-5 (Ad5) was used as the vector. First, A549 human lung carcinoma cells were transduced with various doses of Ad5-N. Twenty-four hours later, whole cell lysates were harvested. IB indicated that transduction with 100 MOI (multiplicity of infection) Ad5-N led to maximal S2NP expression (Figure 1A). In this scenario, A549 cells were incubated with MitoSOX™ red reagent 24 h after transduction with 100 MOI Ad5 and Ad5-N. Flow cytometric analysis revealed that Ad5-N-transduced cells exhibited higher level of mitochondrial ROS than Ad5-transduced counterparts (Figure 1B).

Oxidative stress triggers the phosphorylation of stress-induced protein kinases, namely, c-Jun N-terminal protein kinase (JNK) together with p38.[21] Indeed, IB revealed elevated levels of JNK phosphorylation at Tyr185 and Thr183 and p38 phosphorylation at Tyr182 and Thr180, indicators of their activation, upon the expression of FLAG-tagged S2NP (Figure 1C).

3.2 | Bulk RNA sequencing suggests of aberrant redox state of the electron transport chain upon the expression of S2NP

To investigate the underlying mechanism(s) by which S2NP enhances the level of mitochondrial ROS, Ad5- and Ad5-N-transduced A549 cells were subjected to bulk RNA sequencing. As expected, Ad5-N-transduced A549 cells showed altered transcriptome, as compared with Ad5-transduced counterparts (Figure 2A). Strikingly, mRNA levels of all mitochondrially encoded proteins were upregulated in Ad5-N-transduced A549 cells (Figure 2B). Similar phenomena were observed for *MT-CYB*, *MT-ND1*, *MT-ATP6*, *MT-CO2*, and *MT-CO1* with quantitative RT-PCR (Figure 2C). In line with this, GO_BP enrichment assessments for DEGs highlighted "oxidative phosphorylation," "ATP synthesis coupled electron transport," "respiratory electron transport chain," and so forth (Figure 2D).

### 3.3 | The expression of S2NP enhances the activity of complexes I and III

Since bulk RNA sequencing suggests that the expression of S2NP impairs ATP synthesis coupled electron transport, we measured ATP production in Ad5- and Ad5-N-transduced A549 cells. As shown in Figure 3A, when the same number of Ad5- and Ad5-N-transduced
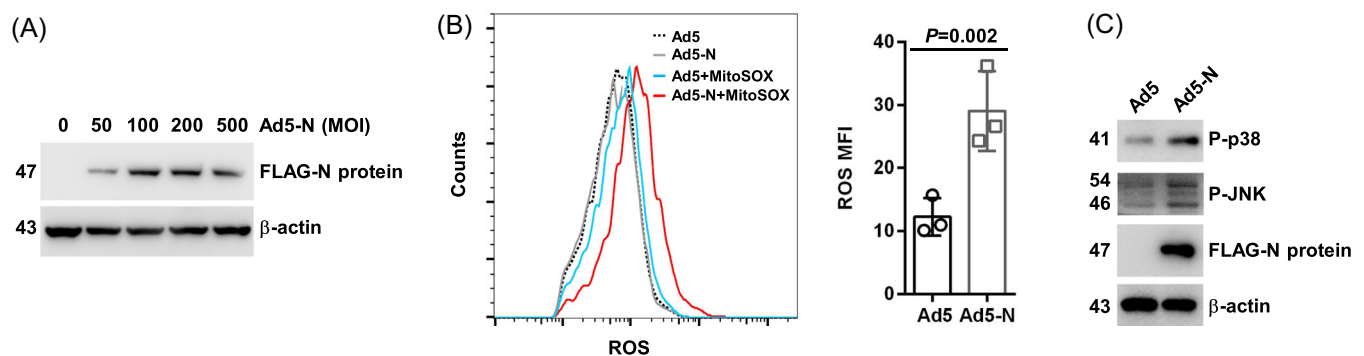
FIGURE 1 S2NP expression enhances the level of mitochondrial ROS. (A) A549 human lung carcinoma cells were transduced with different doses of recombinant adenovirus type-5 expressing FLAG-tagged S2NP (Ad5-N). Twenty-four hours later, whole cell lysates were harvested and subjected to IB with antibodies for FLAG and β-actin. (B) A549 cells were transduced with 100 MOI Ad5 and Ad5-N. Twenty-four hours later, cells were subjected to mitochondrial ROS staining with 0.5 μM MitoSOX™ red reagent, followed by flow cytometry analysis. Left, representative flow cytometry plot; right, statistical data of MFI (mean fluorescence level). Data sets reflect two separate runs. (C) A549 cells were transduced using 100 MOI Ad5 and Ad5-N. Twenty-four hours later, cells were subjected to IB with antibodies for phospho-JNK (P-JNK, Thr183/Tyr185), phospho-p38 (P-p38, Thr180/Tyr182), FLAG, and β-actin. Data sets reflect two separate runs. IB, immunoblotting; MOI, multiplicity of infection; ROS, reactive oxygen species.
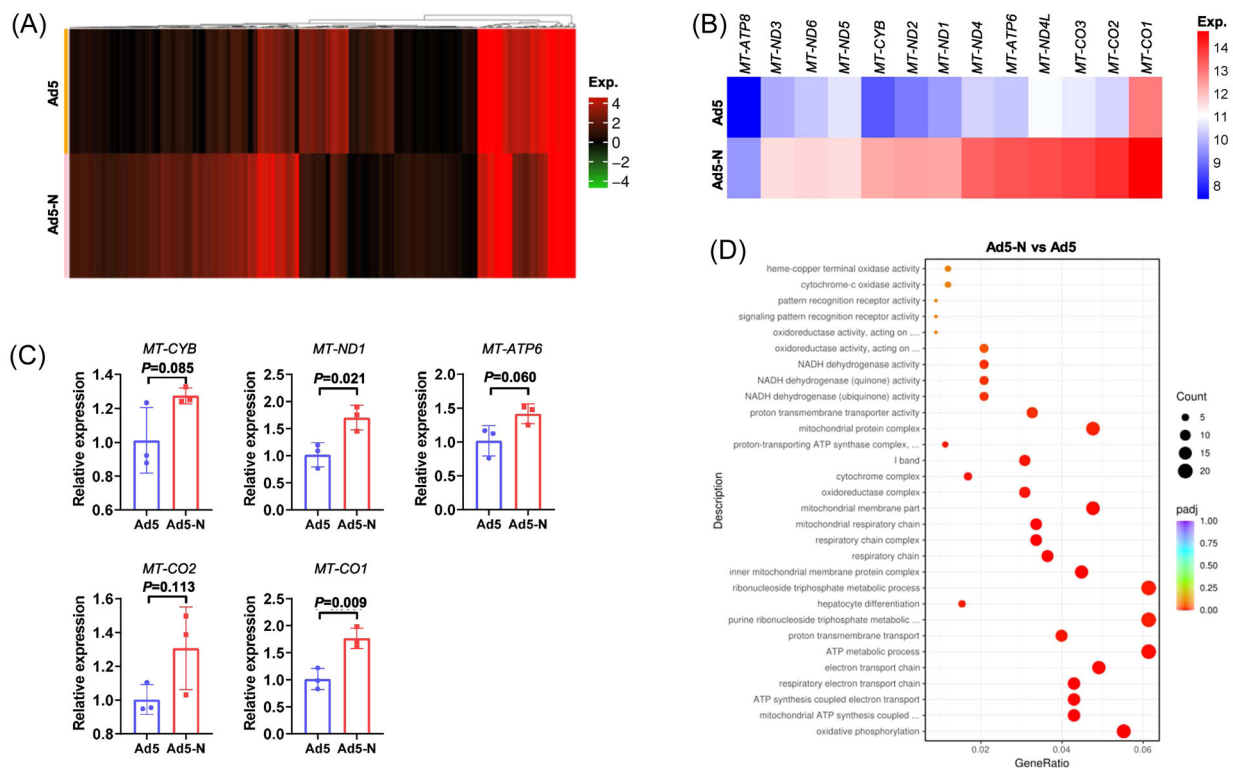
FIGURE 2 Bulk RNA sequencing suggests of aberrant redox state of the electron transport chain upon S2NP expression. (A) A549 cells were transduced using 100 MOI Ad5 and Ad5-N. Twenty-four hours later, cells were subjected to bulk RNA sequencing. Heatmap of the transcriptomes of Ad5- and Ad5-N-transduced A549 cells. (B) FPKMs of mitochondrially encoded proteins as revealed by bulk RNA sequencing in (A). (C) Ad5- and Ad5-N-transduced A549 cells were subjected to quantitative RT-PCR to examine the relative expression of MT-CYB, MT-ND1, MT-ATP6, MT-CO2, and MT-CO1. (D) The top 30 enriched GO_BP terms as revealed by bulk RNA sequencing in (A). BP, biological process; GO, gene ontology; MOI, multiplicity of infection.
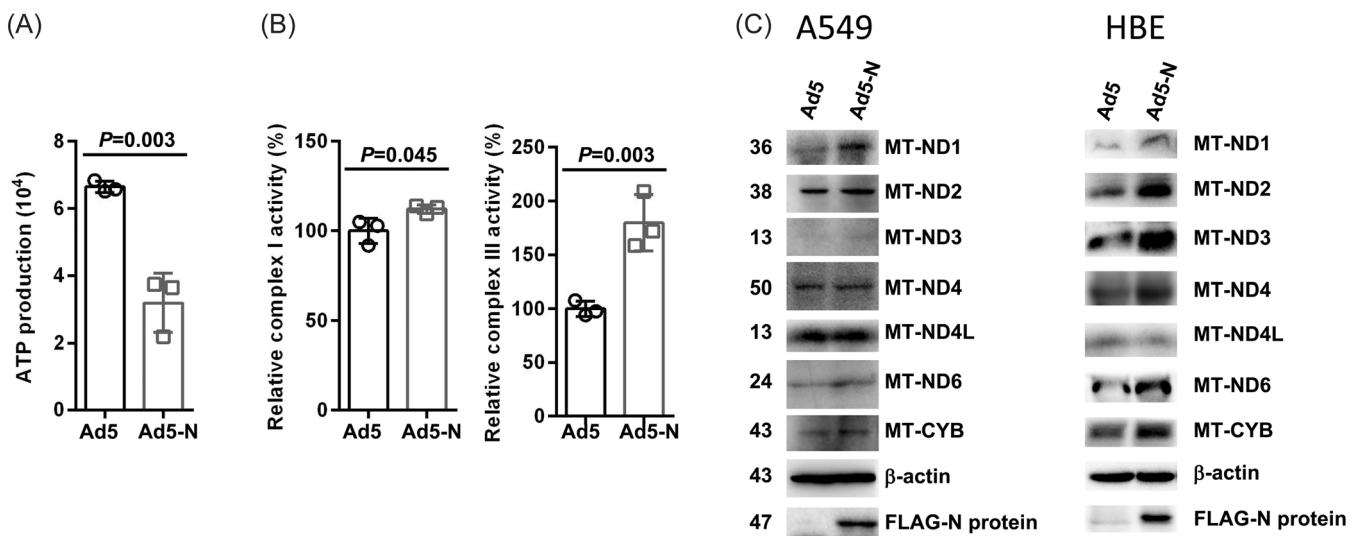
FIGURE 3 S2NP expression enhances complex I and III function. (A) Ad5- and Ad5-N-transduced A549 cells were placed within 96-well plate (5000 cells/well). Once cellular suspensions became attached 12 h later, ATP production was measured with the ATPlite™ assay system. Data sets reflect two separate runs. (B) Cellular extracts or mitochondria were prepared from Ad5- and Ad5-N-transduced A549 cells, followed by measuring the activity of complex I or complex III, respectively. Data sets reflect two separate runs. (C) Ad5- and Ad5-N-transduced A549/HBE cells were subjected to IB with antibodies against MT-ND1, MT-ND2, MT-ND3, MT-ND4, MT-ND4L, MT-ND6, MT-CYB, FLAG, and β-actin. Data sets reflect three separate runs.

A549 cells were seeded, the ATP level of Ad5-N-transduced A549 cells was lower than that of Ad5-transduced counterparts. Thus, the expression of S2NP hinders ATP production. Electron leakage during ATP synthesis mainly occurs at complexes I and III. Thus, we set out to measure their activity. As expected, the expression of S2NP led to weakly enhanced complex I activity and dramatically enhanced complex III activity (Figure 3B). Because mRNA levels of all mitochondrially encoded complex I and III proteins were upregulated in Ad5-N-transduced A549 cells (Figure 2B), we further tried to confirm their upregulated expression with IB. Indeed, the protein levels for MT-ND1, MT-ND2, MT-ND3, MT-ND4, MT-ND6, and MT-CYB were augmented in Ad5-N-transduced A549 cells, as compared with those in Ad5-transduced counterparts, although the protein level of MT-ND4L was unaffected (Figure 3C). Interestingly, we observed similar results in Ad5-N-transfected HBE human bronchial epithelial cells (Figure 3C). Overall, such data sets indicate the upregulation of mitochondrially encoded complex I and III proteins by S2NP protein, which contributes—at least partially—to the upregulation of complex I and III activity.
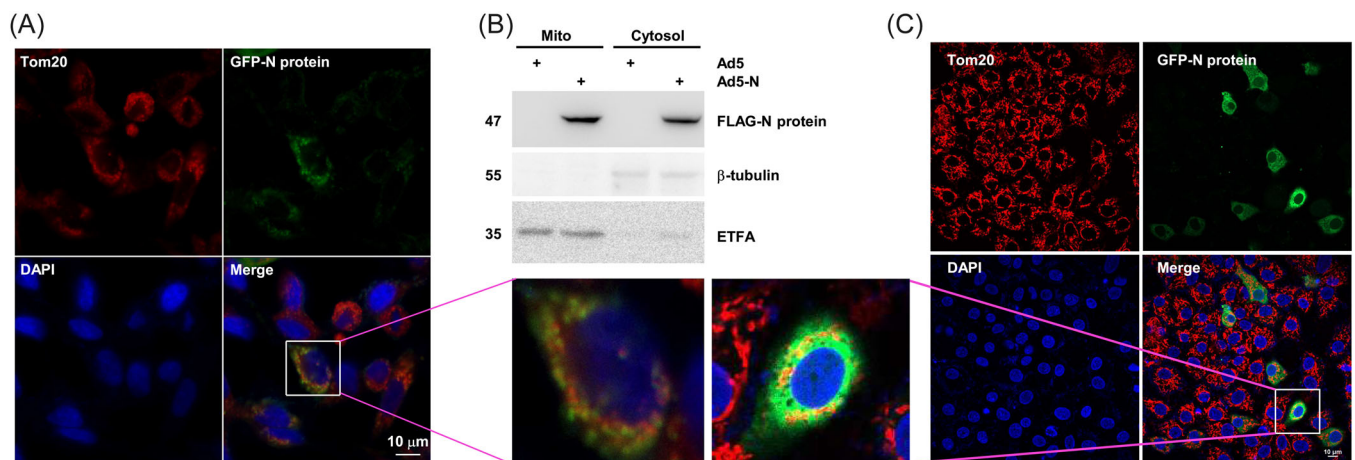
3.4 | S2NP shows significant mitochondrial localization

Notably, the S2NP increases the mRNA and protein levels of mitochondrially encoded complex I and III proteins. In light of this, we investigated whether this protein can enter the mitochondria. In Ad5-N, different promoters drive the expression of S2NP and GFP separately. Therefore, GFP does not reflect the subcellular localization of S2NP in Ad5-N-transduced cells. Therefore, we inserted the sequence encoding S2NP into the pEGFP-N1 plasmid so that GFP is expressed in fusion with S2NP and thereby indicates the subcellular localization of S2NP. A549 cells were transfected with a mammalian expression plasmid encoding GFP-tagged S2NP. Non-direct immunofluorescence assessments demonstrated that the S2NP was primarily cytoplasmic, having a significant portion spread across mitochondria in A549 cells (Figure 4A). To confirm this observation, A549 cells were transduced with Ad5 and Ad5-N. Twenty-four hours later, the cytoplasmic and mitochondrial localization of S2NP was further demonstrated by isolating mitochondria and cytosol, followed by IB (Figure 4B). We also analyzed the subcellular localization of S2NP in HBE human bronchial epithelial cells transfected with a mammalian expression plasmid encoding GFP-tagged S2NP. As expected, the cytoplasmic and mitochondrial localization of S2NP was observed (Figure 4C).

3.5 | S2NP augments the stability of mitochondrial transcription components through the ubiquitin-proteasome system

The 13 mitochondrially encoded proteins are essential for ATP synthesis coupled electron transport.[22] For their transcription, mitochondrial DNA-driven RNA polymerase (POLRMT) binds to promoter elements in a sequence-specific manner, aided by mitochondrial transcription factor A (TFAM) and mitochondrial transcription factor B2 (TFB2M) to initiate the transcription.[22]

FIGURE 4 S2NP shows significant mitochondrial localization. (A) Twenty-four hours after transfection with a mammalian expression plasmid encoding GFP-tagged S2NP, A549 cultures underwent non-direct immunofluorescence assessment using an antibody for mitochondrial marker Tom20, followed by DAPI-counterstaining and eventual confocal microscopic examination (scale bar: 10 µm). (B) A549 cells were transduced using 100 MOI Ad5 and Ad5-N. Twenty-four hours later, subcellular identification for S2NP within A549 cultures was examined by isolation of mitochondria and cytosol and subsequent immunoblotting. ETFA is a mitochondrial marker, whereas β-tubulin is a cytosolic marker. (C) Twenty-four hours after transfection with a mammalian expression plasmid encoding GFP-tagged S2NP, HBE cultures underwent non-direct immunofluorescence assessment using an antibody for mitochondrial marker Tom20, followed by DAPI-counterstaining and eventual confocal microscopic examination (scale bar: 10 µm). MOI, multiplicity of infection.

According to our bulk RNA sequencing data, the mRNA levels of POLRMT, TFB2M, and TFAM remained unchanged with or without the S2NP expression (Figure 5A). However, the protein levels of POLRMT, TFB2M, and TFAM were significantly augmented (Figure 5B). The S2NP is speculated to stimulate or inhibit the degradation of its interacting proteins by the ubiquitin-proteasome.[12] Indeed, endogenous POLRMT, TFB2M, and TFAM coprecipitated with exogenous FLAG-tagged S2NP (Figure 5C). MG132 (proteasome inhibitor) treatment led to higher protein levels of POLRMT, TFB2M, and TFAM in A549 cells (Figure 5D), indicating that these proteins undergo proteasome-dependent degradation in homeostasis. Moreover, the augmentation of POLRMT, TFB2M, and TFAM protein levels by S2NP diminished in the presence of MG132 (Figure 5D), indicating that S2NP blocks the proteasome-dependent degradation of mitochondrial transcription components. Accordingly, the ubiquitination of TFAM in A549 cells was detected with an antibody that can efficiently IP TFAM, which was blocked upon the S2NP expression (Figure 5E). These data support the notion that S2NP promotes the transcription of mitochondrially encoded complex I and III proteins by binding to and stabilizing mitochondrial transcription components.
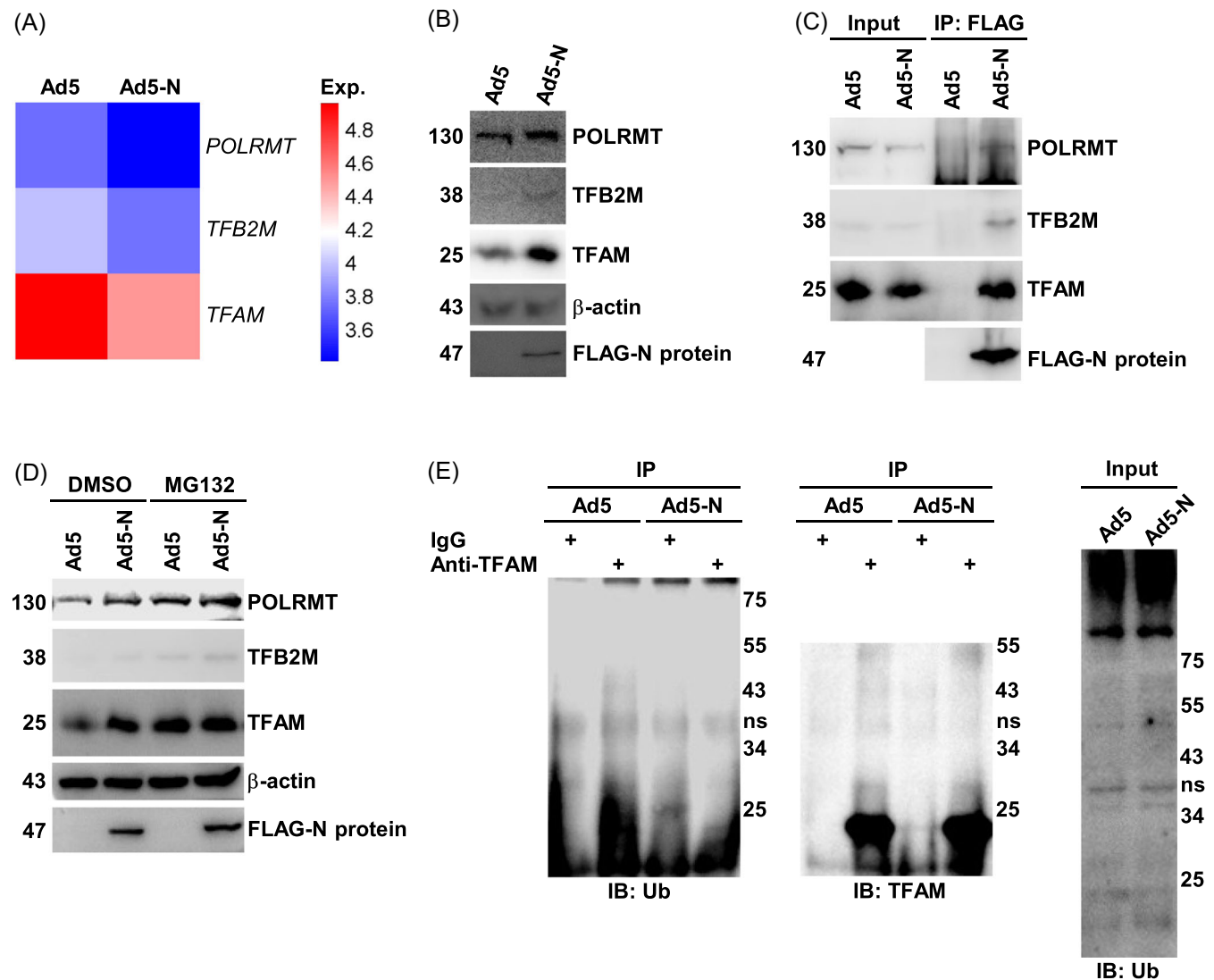
FIGURE 5 S2NP augments the stability of mitochondrial transcription components through the ubiquitin-proteasome system. (A) FPKMs of mitochondrial transcription components as revealed by bulk RNA sequencing in Figure 2A. (B) Ad5- and Ad5-N-transduced A549 cells were subjected to IB with antibodies against POLRMT, TFB2M, TFAM, FLAG, and β-actin. Data sets reflect three separate runs. (C) Ad5- and Ad5-N-transduced A549 cells were subjected to co-IP with an antibody against FLAG, followed by IB with antibodies against POLRMT, TFB2M, TFAM, and FLAG. Please note that the input was adjusted to balance the protein level of POLRMT, TFB2M, and TFAM in Ad5- and Ad5-N-transduced A549 cells. Data sets reflect two separate runs. (D and E) After Ad5- and Ad5-N-transduced A549 cultures were exposed to 20 μM MG132 or equivalent DMSO levels (6 h), cells were directly subjected to IB with antibodies against POLRMT, TFB2M, TFAM, FLAG, and β-actin (D) or the ubiquitination of TFAM was assessed through IB post-IP employing an anti-TFAM antibody or a control IgG antibody (E). co-IP, coimmunoprecipitation.

3.6 | S2NP impairs the activity of antioxidant enzymes with or without detectable interaction

It has been reported that an augmented level of ROS leads to decreased expression of antioxidative enzymes.[23] According to our bulk RNA sequencing data, *CAT, SOD1, SOD2, GPX1, GPX2, GPX3, GPX4,* and *GPX8* mRNAs were readily detected in A549 cells. The expression of S2NP led to lower levels of *SOD1, GPX1, GPX3,* and *GPX4* and a higher level of *GPX2*. Thus, the total FPKMs of *SODs* and *GPXs* partially decreased in Ad5-N-transduced A549 cultures (Figure 6A). Even though quantitative RT-PCR failed to confirm the downregulation of *SOD1*, it confirmed the unchanged levels of *CAT* and *GPX8*, the higher level of *GPX2*, and the lower level of *GPX4* upon S2NP expression (Figure 6B). IB indicated reduced protein expression for SOD1 together with the unchanged protein levels of CAT and GPX8 in Ad5-N-transduced A549 cells (Figure 6C). Thus, the discrepancy of *SOD1* data might result from the low specificity of PCR primers. Measuring the activity of antioxidative enzymes revealed that S2NP partially inhibited SOD and Gpx activity (Figure 6D), in line with the reduced total FPKMs of *SODs* and *GPXs* in Ad5-N-transduced A549 cells (Figure 6A). However, S2NP blocked CAT activity even more potently (Figure 6D), which could not be explained by its expression level (Figure 6A). In this scenario, we set

out to explore whether S2NP interacts with antioxidative enzymes. As shown in Figure 6E, the binding of this protein to CAT, but not SOD1 and GPX8, was detected in A549 cells. Together, these data indicate that S2NP impairs the activity of antioxidant enzymes with or without detectable interaction.

4 | DISCUSSION

Accumulating evidence indicate that SARS-CoV-2 induces mitochondrial damage.[24–26] After SARS-CoV-2 infection, several mitochondrial ribosomal genes and nuclear-encoded complex I component genes are downregulated, whereas apoptosis-inducing genes are upregulated, in human airway epithelial cells.[24,25] Intriguingly, SARS-CoV-2 proteins show heterogeneity in the effects on mitochondrial functions. For example, Nsp7 and Nsp9, but not M protein, promote mitochondrial fission.[24] On the other hand, M protein, but not Nsp7 and Nsp9, reduces mitochondrial permeability transition pore activity.[24] S2NP is multifunctional and is involved in the pathogenesis of COVID-19. This study demonstrates that S2NP augments mitochondrial ROS level through the upregulation of mitochondrially encoded complex I and III proteins. The upregulation of mitochondrially encoded complex I and III
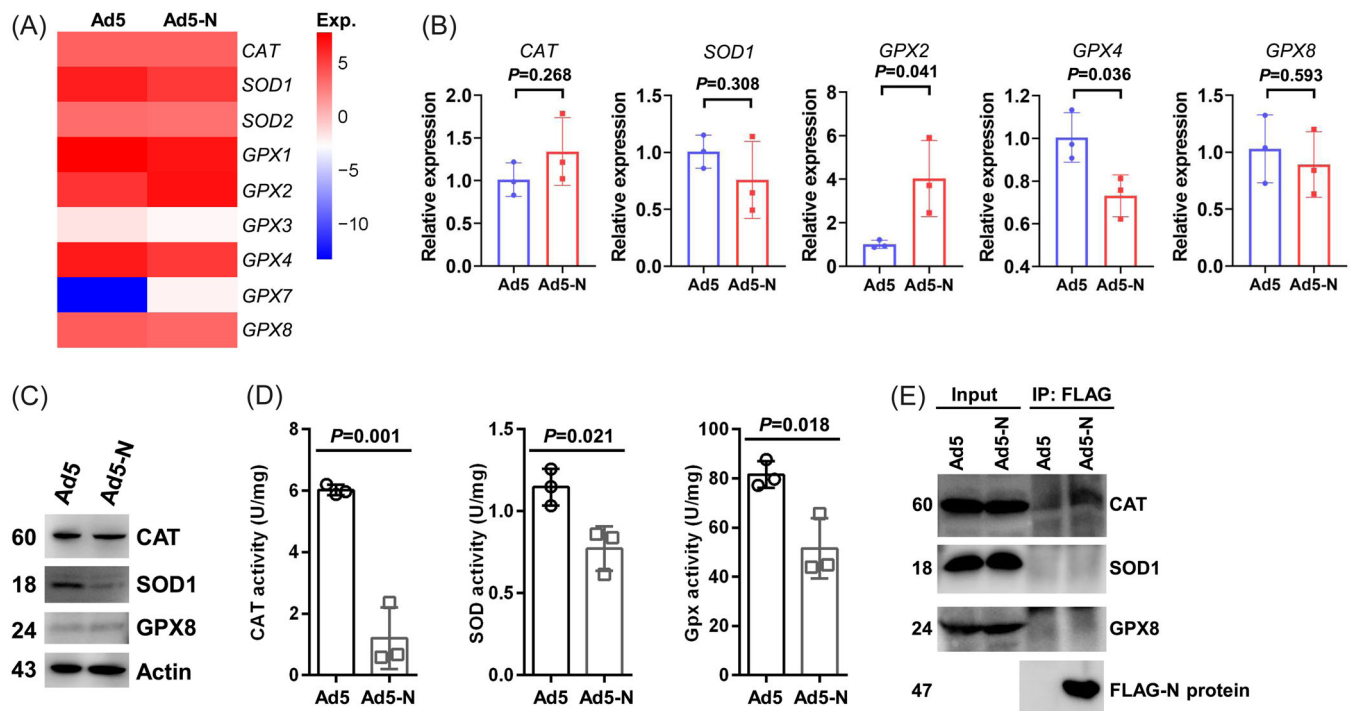
FIGURE 6 S2NP impairs antioxidant enzyme function with or without detectable interaction. (A) FPKMs of *CAT, SODs,* and *GPXs* as revealed by bulk RNA sequencing in Figure 2A. (B) Ad5- and Ad5-N-transduced A549 cells were subjected to quantitative RT-PCR to examine the relative expression of *CAT, SOD1, GPX2, GPX4,* and *GPX8*. (C) Ad5- and Ad5-N-transduced A549 cells were subjected to IB with antibodies against CAT, SOD1, GPX8, FLAG, and β-actin. Data sets reflect three separate runs. (D) Ad5- and Ad5-N-transduced A549 cells were homogenized and subjected to the measurement of CAT, SOD, and Gpx activity. Data sets reflect two separate runs. (E) Ad5- and Ad5-N-transduced A549 cells were subjected to co-IP with an antibody against FLAG, followed by IB with antibodies against CAT, SOD1, GPX8, and FLAG. Please note that the input was adjusted to balance the protein level of CAT, SOD1, and GPX8 in Ad5- and Ad5-N-transduced A549 cells. Data sets reflect two separate runs. CAT, catalase; co-IP, coimmunoprecipitation; Gpx, glutathione peroxidases; SOD, superoxide dismutases.

proteins, however, was not observed in SARS-CoV-2-infected human airway epithelial cells.[24,25] Due to the facility restriction, we can't perform SARS-CoV-2 infection. It remains unclear whether the S2NP amounts expressed in Ad5-N-transduced A549 cells are a realistic reflection of its levels found in cells infected with SARS-CoV-2. Maybe S2NP amounts expressed in the A549 cells following transduction are much higher than their levels in SARS-CoV-2-infected human airway epithelial cells, which makes the difference. Despite that, considering the downregulation of mitochondrial ribosomal genes but the unchanged expression of mitochondrially encoded complex I and III proteins in SARS-CoV-2-infected human airway epithelial cells,[24,25] it is reasonable to propose that S2NP counteracts against other SARS-CoV-2 proteins to maintain the levels of mitochondrially encoded complex I and III proteins.

S2NP can interact with various proteins and modulate their stability, subcellular localization, or activity.[12] A previous study has revealed that in human airway epithelial cells infected by HCoV-OC43, another human-infecting β-Coronavirus family constituent, N protein colocalizes with the mitochondrial outer membrane.[24] Here, we further show that S2NP can enter the mitochondrion and bind to mitochondrial transcription components POLRMT, TFB2M, and TFAM. Its interaction with mitochondrial transcription components is correlated with augmented protein levels of POLRMT, TFB2M, and TFAM. In our hands, the augmentation of POLRMT, TFB2M, and TFAM protein levels by S2NP can be reversed by the proteasome inhibitor MG132, which excludes the possibility that S2NP enhances the translation of mitochondrial transcription components. By contrast, these findings suggest that S2NP blocks the proteasome-dependent degradation of mitochondrial transcription components. Furthermore, we show TFAM undergoes ubiquitination which is blocked by S2NP. Thus, it is very likely that this protein stabilizes mitochondrial transcription components by directly binding to them. This notion can be firmly confirmed if S2NP truncate(s) defective binding to mitochondrial transcription components lose the ability to augment the protein levels of POLRMT, TFB2M, and TFAM. Thus, the interaction domains between S2NP and mitochondrial transcription components should be carefully identified in the future. In addition to stabilizing mitochondrial transcription components, S2NP may also facilitate the assembly of initiation complexes for the transcription of mitochondrially encoded proteins. Future studies are required to address this issue.

S2NP also binds to CAT. Its expression shows no effect on CAT protein level but blocks CAT activity. Similar to the situation for mitochondrial transcription components, it is essential to identify the interaction domains between S2NP and CAT to clarify whether it inhibits CAT activity by directly binding to it. Without detectable interaction, this protein also partially inhibits SOD and Gpx activity with partially reduced total FPKMs of *SODs* and *GPXs*. Since an augmented level of ROS leads to decreased expression of antioxidative enzymes,[23] most likely ROS mediates the effects of S2NP on SOD and Gpx expression and activity.

Together, our study indicates that S2NP promotes mitochondrial ROS production through various mechanisms.

AUTHOR CONTRIBUTIONS

Haiyun Yu, Fang Zheng, and Chaohong Liu designed the study. Haiyun Yu, Lu Yang, Zhennan Han, Xiaoyu Zhou, Zihan Zhang, Tianli Sun, and Fei Guan performed the experiments. Haiyun Yu, Jingzhi Yang, and Lu Yang analyzed bulk RNA-sequencing data. Jungang Xie provided HBE cells and critical suggestions. Haiyun Yu and Chaohong Liu drafted the manuscript. All authors read and contributed to the editing of the manuscript and approved the final version.

ACKNOWLEDGMENTS

CONFLICT OF INTEREST STATEMENT

The authors declare no conflict of interest.

DATA AVAILABILITY STATEMENT

The data that support the findings of this study are available from the corresponding author upon reasonable request. All data, materials, and methods are included in the article.

ORCID

Jungang Xie http://orcid.org/0000-0001-9037-3027
Chaohong Liu http://orcid.org/0000-0001-7028-4625

REFERENCES

1. Tavassolifar MJ, Aghdaei HA, Sadatpour O, et al. New insights into extracellular and intracellular redox status in COVID-19 patients. *Redox Biol*. 2023;59:102563.
2. Hosseini A, Stojkov D, Fettrelet T, Bilyy R, Yousefi S, Simon HU. Transcriptional insights of oxidative stress and extracellular traps in lung tissues of fatal COVID-19 cases. *Int J Mol Sci*. 2023;24:2646.
3. Suresh V, Behera P, Parida D, et al. Therapeutic role of N-acetyl cysteine (NAC) for the treatment and/or management of SATS-CoV-2-induced lung damage in hamster model. *Eur J Pharmacol*. 2023;938:175392.
4. Shadel GS, Horvath TL. Mitochondrial ROS signaling in organismal homeostasis. *Cell*. 2015;163(3):560-569.
5. Leavy O. Regulating ROS. *Nat Rev Immunol*. 2014;14(6):357.
6. Finkel Y, Mizrahi O, Nachshon A, et al. The coding capacity of SARS-CoV-2. *Nature*. 2021;589:125-130.
7. Hoffmann M, Kleine-Weber H, Schroeder S, et al. SARS-CoV-2 cell entry depends on ACE2 and TMPRSS2 and is blocked by a clinically proven protease inhibitor. *Cell*. 2020;181:271-280.
8. Patel VB, Zhong JC, Grant MB, Oudit GY. Role of the ACE2/angiotensin 1–7 axis of the renin–angiotensin system in heart failure. *Circ Res*. 2016;118(8):1313-1326.
9. Griendling KK, Minieri CA, Ollerenshaw JD, Alexander RW. Angiotensin II stimulates NADH and NADPH oxidase activity in cultured vascular smooth muscle cells. *Circ Res*. 1994;74(6):1141-1148.

10. Savastano A, Ibáñez de Opakua A, Rankovic M, Zweckstetter M. Nucleocapsid protein of SARS-CoV-2 phase separates into RNA-rich polymerase-containing condensates. *Nat Commun*. 2020;11:6041.

11. Fehr AR, Perlman S. Coronaviruses: an overview of their replication and pathogenesis. *Methods Mol Biol*. 2015;1282:1-23.

12. Yu H, Guan F, Miller H, Lei J, Liu C. The role of SARS-COV-2 nucleocapsid protein in antiviral immunity and vaccine development. *Emerg Microbes Infect*. 2023;12(1):e2164219.

13. He J, Huang JR, Zhang YL, Zhang J. SARS-CoV-2 nucleocapsid protein intranasal inoculation induces local and systemic T cell responses in mice. *J Med Virol*. 2021;93:1923-1925.

14. Xie P, Zhang M, He S, et al. The covalent modifier Nedd8 is critical for the activation of Smurf1 ubiquitin ligase in tumorigenesis. *Nat Commun*. 2014;5:3733.

15. Wang J, Tang R, Lv M, Zhang J, Shen B. Selective unresponsiveness to the inhibition of p38 MAPK activation by cAMP helps L929 fibroblastoma cells escape TNF-α-induced cell death. *Mol Cancer*. 2010;9:6.

16. Niu C, Yu J, Zou T, et al. Identification of hematopoietic stem cells residing in the meninges of adult mice at steady state. *Cell Rep*. 2022;41:111592.

17. Lundin A, Hasenson M, Persson J, et al. Estimation of biomass in growing cell lines by ATP assay. *Methods Enzymol*. 1986;133:27-42.

18. Aebi H. Catalase in vitro. *Methods Enzymol*. 1984;105:121-126.

19. Perry JJP, Shin DS, Getzoff ED, Tainer JA. The structural biochemistry of the superoxide dismutases. *Biochimica et Biophysica Acta (BBA)-Proteins Proteomics*. 2010;1804:245-262.

20. Mannervik B. Glutathione peroxidase. *Methods Enzymol*. 1985;113:490-495.

21. Benhar M, Engelberg D, Levitzki A. ROS, stress-activated kinases and stress signaling in cancer. *EMBO Rep*. 2002;3(5):420-425.

22. Gustafsson CM, Falkenberg M, Larsson NG. Maintenance and expression of mammalian mitochondrial DNA. *Annu Rev Biochem*. 2016;85:133-160.

23. Furukawa S, Fujita T, Shimabukuro M, et al. Increased oxidative stress in obesity and its impact on metabolic syndrome. *J Clin Invest*. 2004;114(12):1752-1761.

24. Archer SL, Dasgupta A, Chen KH, et al. SARS-CoV-2 mitochondriopathy in COVID-19 pneumonia exacerbates hypoxemia. *Redox Biol*. 2022;58:102508.

25. Singh K, Chen YC, Hassanzadeh S, et al. Network analysis and transcriptome profiling identify autophagic and mitochondrial dysfunctions in SARS-CoV-2 infection. *Front Genet*. 2021;12:599261.

26. Mandò C, Savasi VM, Anelli GM, et al. Mitochondrial and oxidative unbalance in placentas from mothers with SARS-CoV-2 infection. *Antioxidants*. 2021;10:1517.

SUPPORTING INFORMATION

Additional supporting information can be found online in the Supporting Information section at the end of this article.